

# Scattering analysis of the indium-tin-oxide (ITO) nanowhiskers on ITO film substrate for thin film solar cell

Hsiao-Wei Liu<sup>a</sup>, Chia-Hua Chang<sup>a</sup>, Chien-chung Lin<sup>b</sup> and Peichen Yu<sup>a\*</sup>

<sup>a</sup> Department of Photonics and Institute of Electro-Optical Engineering, National Chiao Tung University, Hsinchu 30010, Taiwan

<sup>b</sup> Institute of Photonic System, National Chiao Tung University, Tainan 711, Taiwan, R. O. C.  
E-Mail: [yup@faculty.nctu.edu.tw](mailto:yup@faculty.nctu.edu.tw)

## ABSTRACT

Light trapping techniques such as textured interfaces and highly reflective back contacts are important to thin-film solar cells. Scattering at rough interfaces inside a solar cell leads to enhanced absorption due to an increased optical path length in the active layers, which is generally characterized by a haze ratio. In this work, we demonstrate the measured haze characteristics of indium tin oxide nano-whiskers deposited on an ITO-coated glass substrate. A theoretical model based on a modified Mie theory is also employed to analyze the scattering effects of nano-whiskers. Instead of spherical model, a cylindrical condition is imposed to better fit the shapes of the whiskers. The calculated haze-ratio of an ITO whisker layer matches the measurement closely.

**Keywords:** ITO whisker, haze ratio, Mie theory

## 1. INTRODUCTION

The power conversion efficiency (PCE) of thin film solar cell depends on the effective light absorption, which can be improved by light trapping mechanism in broadband wavelength range [1]. The high scattering efficiency of incident light will increase the optical path and enhance the light absorption in thin film solar cell. Conventionally, the transmission scattering is designed at the top surface, which can scatter the incident light and distribute the light field in the solar active layer. In experiment, the capability of scattering could be defined by the haze ratio where:

$$\text{Haze} = 100\% \times \left( 1 - \frac{T_{\text{specular}}}{T_{\text{total}}} \right) \quad (1)$$

With this definition, the scattering capability of the solar cell can be easily evaluated by this haze ratio of the surface. In the past, micro-scale surface structures were applied to raise the scattering capability. However, the micro structure would increase the haze-ratio but reduce the total transmittance due to the surface reflection, which in turn decreases the photons absorption. On the other hand, the nano-scale structure for scattering layer has shown superior properties for both antireflection and scattering efficiency [2]. In our research, the scattering characteristics of the nano-scale whisker layer on transparent substrate were investigated. The whiskers were fabricated by electron beam evaporation system. We demonstrate the measured haze characteristics of novel indium tin oxide (ITO) nano-whiskers deposited on an ITO-coated glass substrate. The ITO nano-whiskers for scattering layer have shown superior properties for both antireflection and scattering efficiency. Moreover, as ITO is a widely used transparent conductive oxide material and the growth technique involves only deposition in low temperature, it is very appealing to employ nano-whiskers in thin-film solar cells as light trapping textures.

Then, we attempted to construct an equivalent sphere model to fit the haze ratio and analysis characteristics of ITO whisker. With a correct model, we can decide the scattering efficiency by designing the structure and shape size. The scattering effect will be discussed in the later with the model fitting results.

## 2. EXPERIMENTAL

The nano-whiskers were deposited on an ITO coated glass substrate using electron-beam evaporation. The glass is attached to a holder, which was tilted at a deposition angle of  $70^\circ$  with respect to the incident vapor flux. The system is equipped with seven holders which circle around the center of the chamber at a speed of 10 rpm during deposition. The target source contained 5 wt %  $\text{SnO}_2$  and 95 wt %  $\text{In}_2\text{O}_3$  and was placed on the bottom center of the chamber. At the beginning of the evaporation, the chamber pressure was first pumped down to  $\sim 10^{-6}$  torr, followed by the introduction of a nitrogen flow rate at 1 sccm to create an oxygen-deficient atmosphere. During growth, the chamber was stabilized at  $260^\circ\text{C}$  and  $\sim 10^{-4}$  Torr with a deposition rate of 0.15 nm/sec for various deposition times.

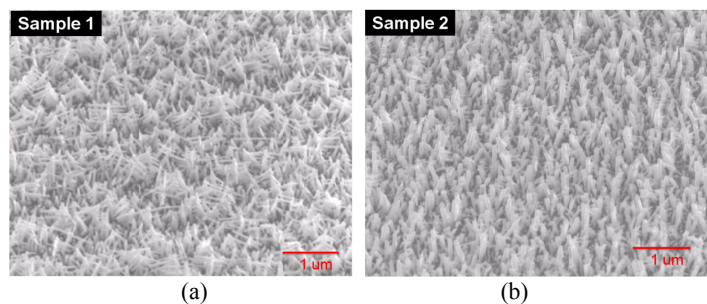


Fig.1 The scanning electron microscopy (SEM) image of the ITO nano-whiskers with different deposition time: (a) 22.2 minutes (b) 16.7minutes.

Figure 1 shows the scanning electron microscopic (SEM) images of the ITO nano-whiskers with two different deposition times: (a) 22.2 minutes, (b) 16.7 minutes, showing the formation of nano-whiskers, which includes a central trunk with a diameter 40~50 nm and several branches on the sides, where the nano-whiskers are randomly distributed on the ITO coating glass substrate. And a longer deposition time results in a higher density of whiskers.

In these structures, the growth mechanism presumably involves a tin-induced self-catalytic vapor-liquid-solid (VLS) [3] process, which is still under investigation. In theory, the growth of ITO nano-whiskers can be divided into three steps, as shown in figure 2. The first step is nucleation, where ITO molecules evaporated from the target form a thin film with a liquid phase on the surface due to oxygen deficiency [4]. The liquid drops consist of an In-Sn-O ternary phase at which  $\text{In}_2\text{O}_3$  nuclei grow into the center and leave the Sn-rich liquid phase on the surface [5]. The high Sn composition lowers the melting point on the surface, which can absorb vapor molecules in the liquid phase continuously. The second step is the rod growth. The Sn-rich liquid phase is supersaturated by the vapor molecules, giving rise to  $\text{In}_2\text{O}_3$  precipitates. The  $\text{In}_2\text{O}_3$  crystalline cores grow along the lattice direction which forms a trunk to reduce the free energy of the liquid-solid system. The concentration of Sn in the core becomes much lower than the liquid surface. Finally, a branch grows from the  $\text{In}_2\text{O}_3$  trunk by breaking through the Sn-rich liquid surface, forming a whisker structure. The branch is composed of crystalline  $\text{In}_2\text{O}_3$  without any core-shell structures.

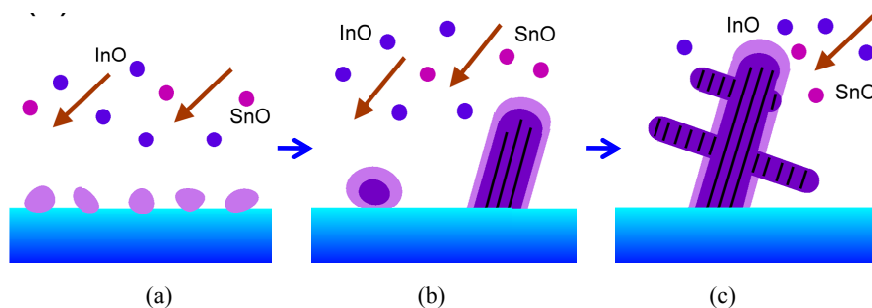


Fig.2 growth mechanism of ITO whiskers breaks into three main step: (a) the nucleation, (b) rod growth, (c) branches, where a Sn-induced self-catalyst is the dominant growth mechanism.

After the nano-structure was grown, we can use the regular Haze measurement setup to evaluate its light-scattering capability. The instrument of U-4100 UV-Visible-NIR Spectrophotometer with a 6-cm diameter integrated sphere was used to characterize the scattered light following the standard ASTM D1003-95

### 3. MIE THEORY WITH CYLINDRICAL ROD

In the ordinary Mie theory, the shape of scattering particle is spherical. In our case, however, the nanowhisker is nowhere close to spherical shape, and so a better simulation should be obtained by using cylindrical particles in modified Mie theory. There have been some efforts in the past to solve the Mie scattering for particles with non-spherical shapes. Shapes like cylinders, spheroids, etc., are common in nature, such as ice pellets, aerosol pollutants, and even organic tissues. Equivalent volume-to-surface-ratio spheres [10], and Mie approximation [11][12] have been proposed as a possible solution. In this paper, we adapt the Mie approximation as our major method to solve the problem.

In the scattering event of a infinitely-long cylinder shown in Fig. 2, the electromagnetic excitation can strike the long axis of the cylinder with an angle of  $\zeta$ . In the regular Mie theory, we need to find out the scattering coefficient, and scattering cross section such that we can calculate the attenuation coefficient [12]. Similar treatment needs to be carried out in the cylindrical case. The scattered EM field are written in the series form of the generating functions[12]:

$$E_{sca} = \sum_{n=1}^{\infty} (a_n M_n + b_n N_n) \quad (2)$$

, where  $a_n$  and  $b_n$  are the scattering coefficients, and  $M_n$  and  $N_n$  are the generating functions that can satisfy the scalar wave equation in polar coordination [12]. The coefficients can be determined by the Maxwell equations and the expansion of the scattered EM field [12]. And if we assume the electric field is perpendicular to the axis of the cylinder, we can obtain the scattering coefficients like [11]:

$$a_n = \frac{C_n V_n - B_n D_n}{W_n V_n + i D_n^2}; b_n = \frac{W_n B_n + C_n D_n}{W_n V_n + i D_n^2} \quad (3)$$

Where

$$\left. \begin{aligned} D_n &= n \cos \zeta \eta J_n(\eta) H_n^{(1)}(\xi) \left(\frac{\xi^2}{\eta^2} - 1\right); B_n = \xi \left(m^2 \xi J_n'(\eta) J_n(\xi) - \eta J_n(\eta) J_n'(\xi)\right) \\ C_n &= n \cos \zeta \eta J_n(\eta) J_n(\xi) \left(\frac{\xi^2}{\eta^2} - 1\right); V_n = \xi \left(m^2 \xi J_n'(\eta) H_n^{(1)}(\xi) - \eta J_n(\eta) H_n^{(1)\prime}(\xi)\right) \\ W_n &= i \xi \left(\eta J_n'(\eta) H_n^{(1)\prime}(\xi) - \xi J_n'(\eta) H_n^{(1)}(\xi)\right) \\ \xi &= x \sin \zeta; \eta = x \sqrt{m^2 - \cos^2 \zeta} \end{aligned} \right\} \quad (4)$$

and  $J_n(x)$ ,  $H_n(1)(x)$  are the Bessel function of the 1st order, and 3rd order,  $x$  is  $2\pi a/\lambda$ ,  $a$  is the radius of the cylinder, and  $m$  is the complex refractive index of the cylinder material. If the electric field is parallel to the axis of the cylinder, a similar set of formula can also be found[11][12]. The scattering efficiency factor  $Q_i$  ( $i=ext$ , and  $sca$ , for extinction and scattering, respectively) can then be calculated through the summation of  $a_n$  and  $b_n$  [12]:

$$\left. \begin{aligned} Q_{sca} &= \frac{\lambda}{\pi m_1 a} \left[ |b_0|^2 + 2 \sum_{n=1}^{\infty} (|b_n|^2 + |a_n|^2) \right] \\ Q_{ext} &= \frac{\lambda}{\pi m_1 a} \operatorname{Re} \left\{ b_0 + 2 \sum_{n=1}^{\infty} b_n \right\} \end{aligned} \right\} \quad (5)$$

, where  $a$  is the radius of the cylinder and the  $nI$  is the real part of the refractive index of the cylinder. We are assuming the electric field is perpendicular to the axis of the cylinder in this case. If the electric field is parallel to the axis, the coefficients  $a_n$  and  $b_n$  need to be exchanged in their positions in the eq.(5). If the incident light is unpolarized, the

efficiency factors are the average of the coefficients of the two polarizations. Once we find out the scattering efficiency factors, the attenuation coefficients  $\alpha$  can be solved as [11][12]:

$$\alpha_i = NQ_i\pi a^2 \quad (6)$$

, where  $i=\text{ext}$  (extinction) or  $\text{sca}$  (scattering), and  $N$  is the total number of the particles. The haze ratio can then be calculated as  $1-\exp(-\alpha_{\text{sca}}\times d)$ , and  $d$  is the thickness of the scattering medium. Figure 3 shows the calculated haze ratio under different incident angle ( $\zeta$ ) and also at different radii of cylinders. From the plots, we can see the scattering capabilities strongly depends on the physical shapes and orientation of the cylinders.

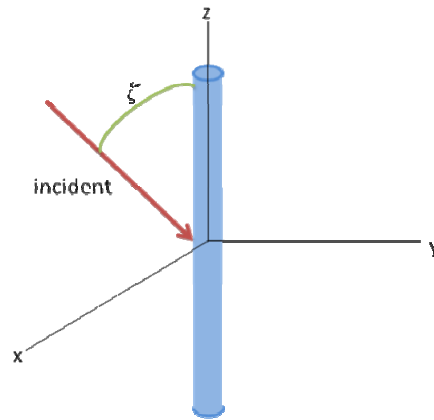


Fig. 3. Schematic diagram of a cylindrical object with incident EM waves.

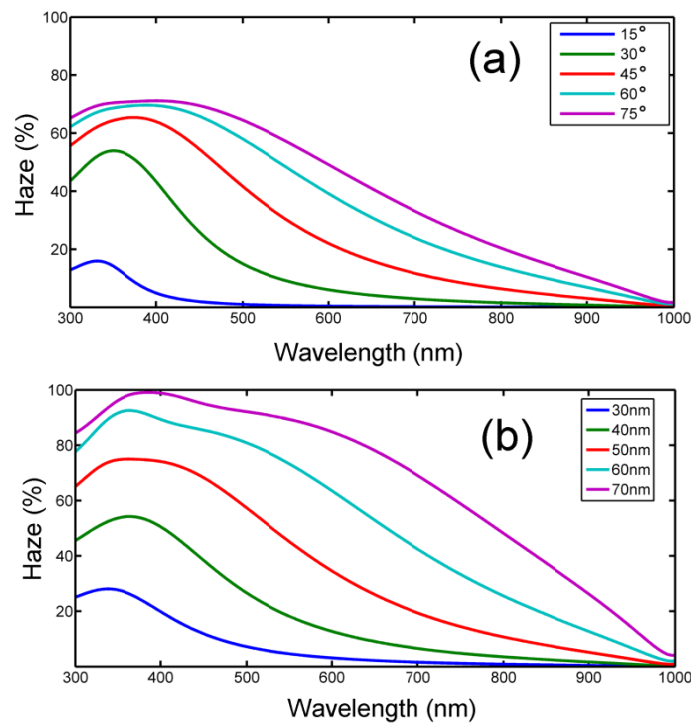


Fig. 4. The calculated haze ratio at (a) different incident angles, and (b) different radius of cylinders.

## 4. RESULTS AND DISCUSSION

From the aforementioned theory, we can use Matlab<sup>TM</sup> and reference to published codes[13] to program the wavelength-dependent haze ratio of nanowhisker and compare the calculation to our measurement. Figure 4 shows our haze fitting of nanowhiskers under various deposition conditions. Two different thickness of ITO nanowhisker films deposited at 260°C were tested and fitted. To better match the real situation, we put a vertical and horizontal orientation mix of cylinders (4:1) in the calculation. The vertical cylinders are tilted in 25° and the horizontal ones are at 75°, both with respect to normal direction of the surface. A illustrative diagram of our simulation model is shown in the inset of Fig. 4. The radii of the cylinders are picked as 28 and 35 nm, which are close to what was observed in the TEM picture[7], and real ITO refractive index was used. The effective thickness in the Mie calculation for both cases are 650nm and 500nm, respectively. These numbers are also obtained from the SEM pictures. A close match was found with the parameters we assigned. Little deviations were found at long wavelength range, which might rise from the randomness of the nanowhisker orientation, and the different sizes of whiskers' radii. At short wavelength, the fine branches of whiskers took effect and drove the scattering away from the ideal infinitely-long cylinder condition.

parameters	Sample 1	Sample 2
<b>The broad rods</b>		
Mean particle radius ,a	35 nm	28 nm
The angle to incident light $\zeta$	25°	25°
<b>The narrow rods</b>		
Mean particle radius ,a	27 nm	20 nm
The angle to incident light $\zeta$	75°	75°
Whicker layer thickness , h	650 nm	500 nm
particles per unit volume , $n$	1/118nm <sup>3</sup>	1/90nm <sup>3</sup>

Table 1 Fitting parameters

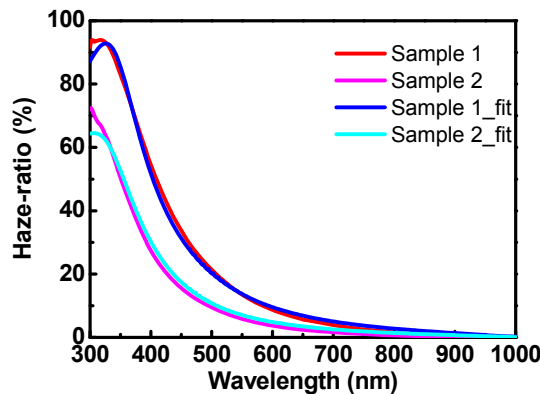


Fig. 5. The measurement data (red and magenta) and the fitted haze ratio (blue and cyan).

## 5. RESULTS AND DISCUSSION

A cylinder-based Mie scattering model was used to calculate the haze ratio of nanowhiskers, and we successfully correlate the physical dimensions to our measurement. The result of curve fitting shows that it is a practical and accurate model for visible light range, but some errors induced by difference of ideal and real case exhibit at short and long wavelength. We believe this Mie model can provide a quick estimate of haze ratio and should be helpful for design of next generation of highly diffused nanostructure.

## ACKNOWLEDGEMENT

The authors are grateful to the National Science Council of the Republic of China, Taiwan, for financially supporting this research. C.C Lin also would like to thank the support of the Contract No. NSC 99-2221-E-009-052-MY3, and NSC 100-3113-E-110-006.

## REFERENCE

- [1] J. Krc, B. Lipovsek, M. Bokalic, A. Campa, T. Oyama, M. Kambe, T. Matsui, H. Sai, M. Kondo, M. Topic, " Potential of thin-film silicon solar cells by using high haze TCO superstrates, " *Thin Solid Film*, 518, 3054-3058, (2010).
- [2] Naoki Taneda, Kunio Masumo, Mika Kambe, Takuji Oyama and Kazuo Sato, "Highly Textured SnO<sub>2</sub> Films For a-Si /  $\mu$ c-Si Tandem Solar Cells," 23rd European Photovoltaic Solar Energy Conference, 1-5 September 2008, Valencia, Spain
- [3] U. Kroll, J. Meier, S. Benagli, et al, "Thin Film Silicon PV: From R&D to Large-Area Production Equipment, " *Amorphous, Nano, and Film Si - Plenary Talk*, 37th IEEE Photovoltaic Specialist Conference, (2011).
- [4] J Müller, B Rech, Jiri Springer, M Vanecek, "TCO and Light Trapping in Silicon Thin Film Solar Cells, " *Solar Energy*. Vol., 77, pp 917-930, 2004.
- [5] D. Domine, F.-J. Haug, C. Battaglia, and C. Ballif, "Modeling of light scattering from micro- and nanotextured surfaces, " *J. Appl. Phys.* 107, 044504 (2010), DOI:10.1063/1.3295902
- [6] Y. J. Lee, D. S. Ruby, D. W. Peters, B. B. McKenzie, J. W. P. Hsu, "ZnO Nanostructures as Efficient Antireflection Layers in Solar Cells," *Nano Lett.* Vol., 8, pp 1501-1505, 2008.
- [7] P. Yu, C. H. Chang, C. H. Chiu, C. S. Yang, J. C. Yu, H. C. Kuo, S. H. Hsu, and Y. C. Chang, "Efficiency Enhancement of GaAs Photovoltaics Employing Indium-Tin-Oxide Nano-Columns", *Advanced Materials*, vol. 21, pp1618-1621, April, 2009. Also highlighted by NPG Nature Asia-Material, April 8, 2009
- [8] C. H. Chang, P. Yu, & C. S. Yang, "Broadband and omnidirectional antireflection from conductive indium-tin-oxide nano-columns prepared by glancing-angle deposition with nitrogen," *Appl. Phys. Lett.* 94, 051114 (2009)
- [9] Chien-Chung Lin, Wei-Lin Liu, and Chi-Ying Hsieh, "Scalar scattering model of highly textured transparent conducting oxide," *J. Appl. Phys.* 109, 014508 (2011), DOI:10.1063/1.3530684
- [10] Thomas C. Grenfell, and Stephen G. Warren, " Representation of a nonspherical ice particle by a collection of independent spheres for scattering and absorption of radiation, " *Journal of Geophysical Research*, Vol. 104, No. D24, p.31697-31709, (1999).
- [11] C. F. Bohren and D. R. Huffman, *Absorption and Scattering of Light by Small Particles*, Willey, New York, 1983. C. Lee, S. Y. Bae, S. Mobasser *et al.*, "A novel silicon nanotips antireflection surface for the micro sun sensor," *Nano Letters*, 5(12), 2438-2442 (2005).
- [12] C Matzler, Matlab functions for Mie Scattering and Absorption, Research Report, University of Bern, 2002